Bioorganic Chemistry 117 (2021) 105463

Contents lists available at ScienceDirect

Bioorganic Chemistry

journal homepage: www.elsevier.com/locate/bioorg

# Clickable, selective, and cell-permeable activity-based probe of human cathepsin B – Minimalistic approach for enhanced selectivity

Ashif I. Bhuiyan [a,h], Pratikkumar Rathod [b], Sarbani Ghoshal [c], Dibyendu Dana [a], Tuhin Das [a], Guoshen Li [a], Anna A. Dickson [a], Faiza Rafi [d], Gopal S. Subramaniam [a], Karl R. Fath [e,f], Suneeta Paroly [d], Emmanuel J. Chang [f,g,h], Sanjai K. Pathak [a,f,h,*]

[a] Queens College of The City University of New York, Chemistry and Biochemistry Department, 65-30 Kissena Blvd, Flushing, NY 11367, USA
[b] Laguardia Community College, 31-10 Thomson Ave, Long Island City, NY 11101, USA
[c] Department of Biological Sc. and Geology, QCC-CUNY, Bayside, NY, USA
[d] Bard High School Early College Queens, 30-20 Thomson Avenue, Long Island City, NY 11101, USA
[e] Queens College of The City University of New York, Department of Biology, 65-30 Kissena Blvd, Flushing, NY 11367, USA
[f] Biochemistry Doctoral Program, The Graduate Center of The City University of New York, 365 5th Ave, New York, NY 10016, USA
[g] York College of the City University of New York, Department of Chemistry, 94-20 Guy R. Brewer Blvd, Jamaica, NY 11451, USA
[h] Chemistry Doctoral Program, The Graduate Center of The City University of New York, 365 5th Ave, New York, NY 10016, USA

ARTICLE INFO

*Keywords:*
Activity-based probe
Cathepsin B probe
KDA-1 probe
Clickable and tagless activity-based probe
Cathepsin B ABP
ABP
Cysteine cathepsins
Activity-based probe of cathepsin B
Cathepsin B

ABSTRACT

Human cathepsin B is a cysteine-dependent protease whose roles in both normal and diseased cellular states remain yet to be fully delineated. This is primarily due to overlapping substrate specificities and lack of unambiguously annotated physiological functions. In this work, a selective, cell-permeable, clickable and tagless small molecule cathepsin B probe, KDA-1, is developed and kinetically characterized. KDA-1 selectively targets active site Cys25 residue of cathepsin B for labeling and can detect active cellular cathepsin B in proteomes derived from live human MDA-MB-231 breast cancer cells and HEK293 cells. It is anticipated that KDA-1 probe will find suitable applications in functional proteomics involving human cathepsin B enzyme.

## 1. Introduction

Human protease biology remains highly relevant in both normal physiology and human disease states, and the members of cysteine cathepsin family enzymes are no exceptions to this.[1–3] Cathepsin B, a critically important and ubiquitously-expressed enzyme with both carboxypeptidase and endopeptidase activities, participates in numerous cellular processes such as cell migration, immune response, apoptosis, autophagy, and ECM degradation.[4,5] In normal cells, cathepsin B activity is tightly regulated by its endogenous protein inhibitors, localization, and post-translational modifications at various levels, such as activation by proteolysis and inhibition by endogenous inhibitory proteins (e.g. cystatin C and A).[6–9] In diseased states however, cathepsin B activities are often dysregulated, thereby promoting serious human diseases, such as highly invasive cancer, liver fibrosis, diabetes, and pancreatitis.[4,10–13] While major efforts are currently targeting cathepsin B for drug development, caution must be exercised.[14] This is primarily due to the lack of precise functional annotations of this enzyme in specific cellular contexts. Individualized roles of cathepsin B therefore must be delineated in specific cellular contexts before significant resources are directed in drug discovery efforts. This problem is further exacerbated since both redundant and unique function of cathepsin B is reported from other homologous members of cathepsin family of enzymes, especially cathepsin L. To cite a few examples of unique functions: During protein digestion from food, while cathepsin B plays a critical role in activating a key protease, trypsin, to initiate the protein degradation signaling cascade, cathepsin L functions to keep the trypsin activation in check;[15–17] Presence of cathepsin B enhances γ-secretase activity in the brain while cathepsin B downregulates it;[18] Similarly both cathepsin B and L may play a role

* Corresponding author at: Queens College of The City University of New York, Chemistry and Biochemistry Department, 65-30 Kissena Blvd, Flushing, NY 11367, USA.
*E-mail address:* Sanjai.Kumar@qc.cuny.edu (S.K. Pathak).

https://doi.org/10.1016/j.bioorg.2021.105463
Received 29 September 2021; Accepted 28 October 2021
Available online 2 November 2021

in promoting autoimmune encephalomyelitis (EAE).[19] An example of redundant and compensatory function is where during inflammation, both cathepsin B and L can independently promote the release and activation of the key cytokine IL-1β.[20] Similarly what precise roles cathepsin B and L play in cardiac signal transduction also remain poorly understood.[21–23]

Activity-based proteomics has emerged as a powerful tool for functional studies of several enzyme classes.[24–28] This technology allows researchers to assess the proteome-wide function of an enzyme based on its 'activity', not just on its cellular expression or mRNA profile alone. The basic design of a typical activity-based probe (ABP) includes (a) A selective targeting electrophilic warhead agent that covalently and irreversibly reacts with a key nucleophilic residue of only the active enzyme form, (b) A detection tag (e.g. a fluorescent group for direct-in-gel visualization, or other epitope, like biotin for immunodetection), and (c) A linker of appropriate size that separates the warhead and the tag so as to promote effective binding to the target enzyme. A few targeted cathepsin B probes have recently been developed and utilized in functional studies (see Fig. 1).[29–32] Among these, the ones reported by Poreba et al. and Pratt et al. utilize the acyloxymethylketone (AOMK) moiety as the electrophilic warhead group (Fig. 1A-B).[29,30] Further, Roth-Konforti et al. developed a chemiluminescence-based cathepsin B probe that utilized Schaap's adamantylidene-dioxetane moiety (Fig. 1C).[33] A prodrug-inspired strategy was adopted by Chaudhury et al. to develop a substrate-based cathepsin B probe (Fig. 1D).[34] While innovative, most reported probes are not exclusively cathepsin B selective. We surmised that this could either be due to (i) more-than-optimal reactivity of the warhead groups utilized, or (ii) design of probes that target several subsites of the substrate binding pockets in order to gain enhanced potency. Given that the key binding pockets surrounding the scicile petidyl bond of the subtrate are relatively similar in several cathepsins (e.g. cathepsin L and S), this may pose a challenge in designing probes that are highly cathepsin B selective.[3] One additional concern often is that previously reported cathepsin B probes contain a sterically 'bulky' detection tag that may thus hinder the probe's ability to either penetrate the living cells, and/or alter the binding affinity toward the target enzyme.[33,35] For development of highly effective cathepsin B ABPs, innovative chemical designs are needed for optimizing the reactivity of an electrophilic warhead, and limiting the steric bulk of the reporter tag group so that its impact is minimal on the initial binding and labeling events.

Herein, we report the development of a highly selective ABP of cathepsin B, KDA-1 (Scheme 1). The design of this probe includes a softer electrophilic fumarate diamide as an electrophilic warhead for promoting selective cathepsin B labeling.[36,37] To maintain selectivity, we employed a 'minimalistic' approach in our design strategy. Our hypothesis was that if we utilized only binding elements of cathepsin B active site that are unique, we may acquire a highly selective probe, although at the cost of potency.[38] We thus analyzed the crystal structure of CA-074 - a known cathepsin B inhibitor - in complex with cathepsin B. We noted that installation of proline residue at the C terminus was essential since it sat in the S2' pocket and its free carboxylate group interacted strongly with the occluding loop (only present in cathepsin B).[39,40] A hydrophobic S1′ pocket of cathepsin B housing Val176, Leu181, Met196, and Trp221 residues also interacted highly favorably with Ile residue. The fumarate diamide warhead was found to be well placed in the S1 pocket, readily accessible to nucleophilic active site Cys29 residue. Finally, a sterically inconspicuous ethinyl group was also engineered at the *N*-terminus for a tagless quantification of labelled cellular cathepsin B using aqueous click chemistry protocols. Using steady-state enzymology experiments, we first demonstrate that KDA-1 inhibits human liver cathepsin B (hcathepsin B) enzyme activity in a time-dependent manner. The inhibition is highly selective toward hCathepsin B. The tandem (MS/MS) mass spectrometry experiments confirm that KDA-1 covalently and irreversibly targets the critically important nucleophilic Cys29 residue of cathepsin B catalytic machinery. Inactivation experiment using active cathepsin B, followed by click chemistry protocol with 5-TAMRA-azide, demonstrate that KDA-1 is an activity-dependent probe. We have also developed a cell-permeable analogue of KDA-1, KDA-1-OMe, suitable for live cell labeling experiments and demonstrate that this molecule reduces cell proliferation of the highly metastatic, cathepsin B-overexpressing human MDA-MB-231 breast cancer cells – a reversal of phenotype consistent with cathepsin B cellular function.[41] Finally, we demonstrate that KDA-1 can detect active hcathepsin B in proteomes derived from human MDA-MB-231 breast cancer cells and HEK293 cells overexpressing hcathepsin B.

## 2. Results and discussion

### 2.1. Synthesis of clickable and tagless cathepsin B probes and their kinetic analysis of inhibition

The synthetic strategy, as outlined in Scheme 1, involved coupling of monomethyl fumarate to propargyl amine followed by methyl ester deprotection to generate intermediate 2. This was then coupled to Ile-Pro-OMe dipeptide, rendering KDA-1-OMe, a 'pro-probe' which is activated by esterases inside cells. Such strategies have been previously implemented in designing cell permeable cathepsin B inhibitors.[42] Finally, saponification of KDA-1-OMe rendered the active form of hcathepsin B probe, KDA-1.

To investigate if KDA-1 was indeed inhibitory towards human cathepsin B, steady state enzymology experiments were performed using purified human liver cathepsin B enzyme (Enzo Life Sciences, Inc.). A dose-dependent loss of human cathepsin B activity was observed, as monitored by the turnover of Z-RR-AMC substrate (Fig. 2A).

To further assess if inhibition was covalent and irreversible, a time-dependent experiment was performed; Inhibition became progressively stronger as KDA-1 incubated with active cathepsin B (Fig. 2B) under pseudo-first order condition (i.e. [KDA-1]≫[Cathepsin B]). The inhibited cathepsin B activity was not recoverable, even after significant dilution, suggesting that inhibition was irreversible (data not shown). The data thus obtained was analyzed using the Kitz-Wilson method, and the kinetic inactivation parameters were obtained: $k_{inact} = 0.05 \pm 0.01$ $min^{-1}$ and $K_i = 76 \pm 21$ μM.[43] Our immediate goal next was to assess the selectlvity of the KDA-1 probe among closely homologous cathepsins, L and S. KDA-1 did not inhibit either cathepsin L or cathepsin S, even after prolonged incubation at 200 μM (Table 1). This suggests that KDA-1 is highly selective toward cathepsin B.

### 2.2. Mass spectrometric analysis of the KDA-1-Human cathepsin B inhibited complex

To confirm that KDA-1 was active site-bound and was indeed targeting the key active site Cys29 residue of human cathepsin B, a mass spectrometric analyses of the inhibited KDA-1/cathepsin B complex was performed. Briefly, the KDA-1/cathepsin B complex was resolved by SDS-PAGE; the cathepsin B band was excised, and in-gel digestion was performed using trypsin. The tryptic digest was subjected to mass spectrometric analysis. A band at 2422.36 Da corresponding to Cys29-containing peptide covalently modified with KDA-1 was observed (Fig. 3A). MS/MS analysis of this mass peak further revealed that the site of modification was the key Cys29 residue, as anticipated (Fig. 3B). These results together confirmed that our probe design strategy was reasonably accurate.

### 2.3. Activity-dependent labeling of purified human cathepsin B

To demonstrate that KDA-1 can be utilized for labeling of purified active human cathepsin B, the activated enzyme was incubated with KDA-1 first, followed by click chemistry with 5-TAMARA-azide fluorophore. Different amounts of clicked-cathepsin B was resolved by SDS-

[A] Cy5-containing AOMK-based Cathepsin B Probe, MP-cB-2

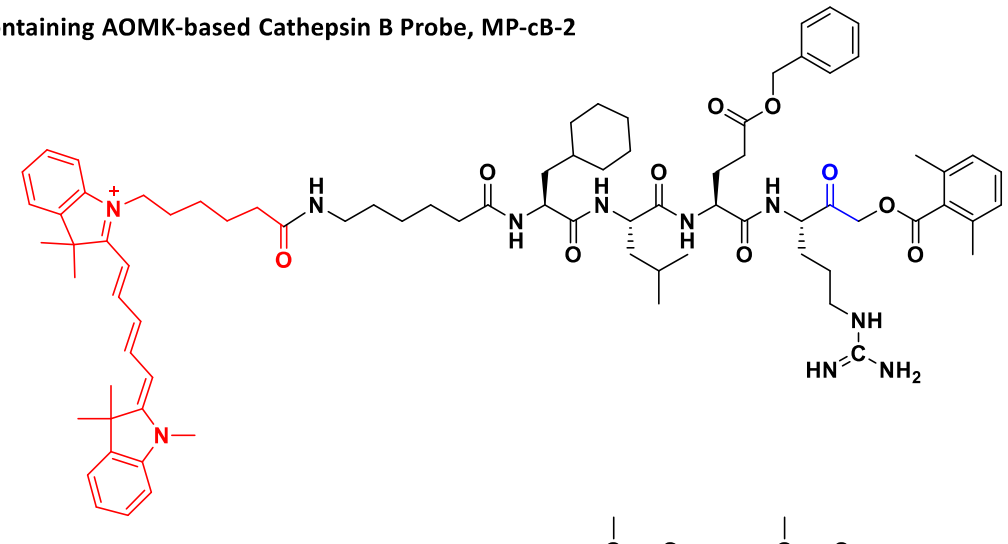

[B] Azide-containing AOMK-based Cathepsin B Probe

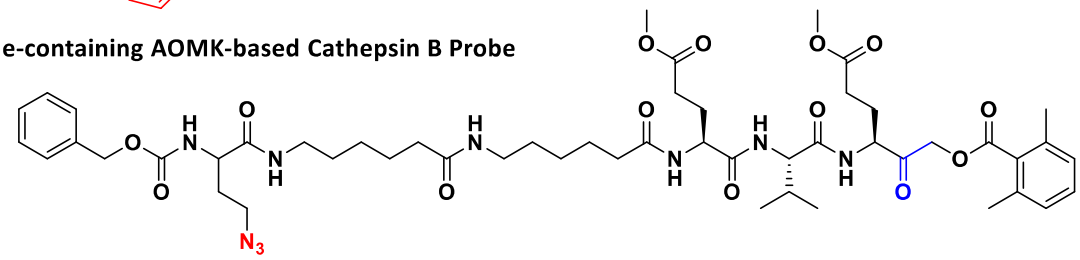

[C] Schaap's Dioxetane-containing Chemiluminescence-based Cathepsin B probe

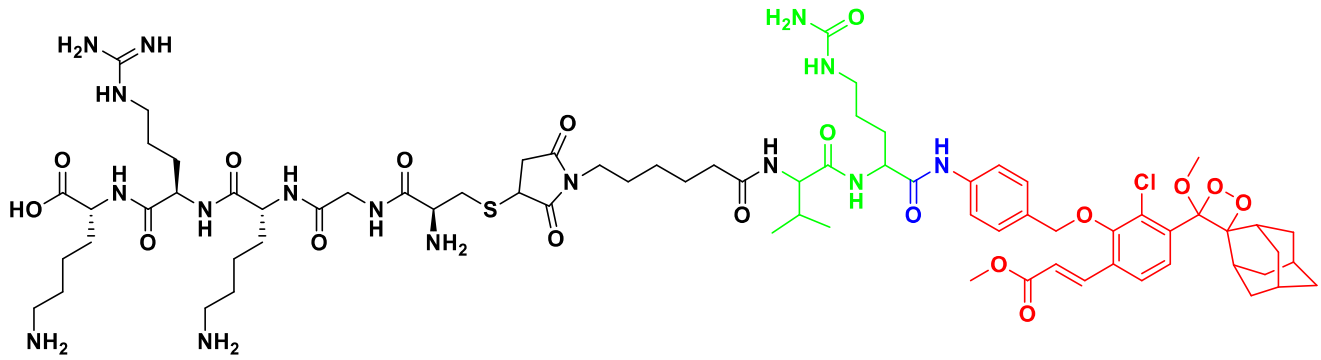

[D] Substrate-based Cathepsin B Probe

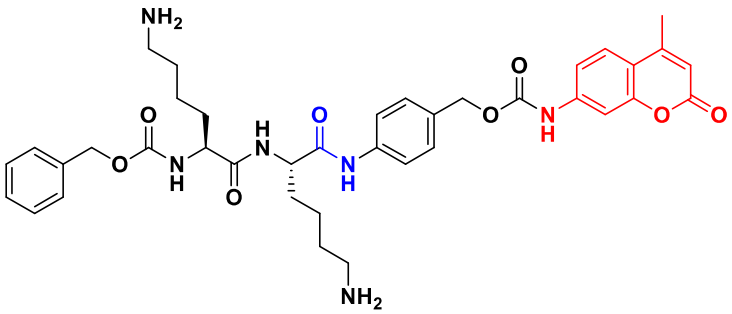

**Fig. 1.** Chemical structures of recently reported cathepsin B probes. Moieties utilized for optical detection of labelled cathepsin B are shown in red. The target position for active site Cys29 residue of cathepsin B is shown in blue. (For interpretation of the references to color in this figure legend, the reader is referred to the web version of this article.)

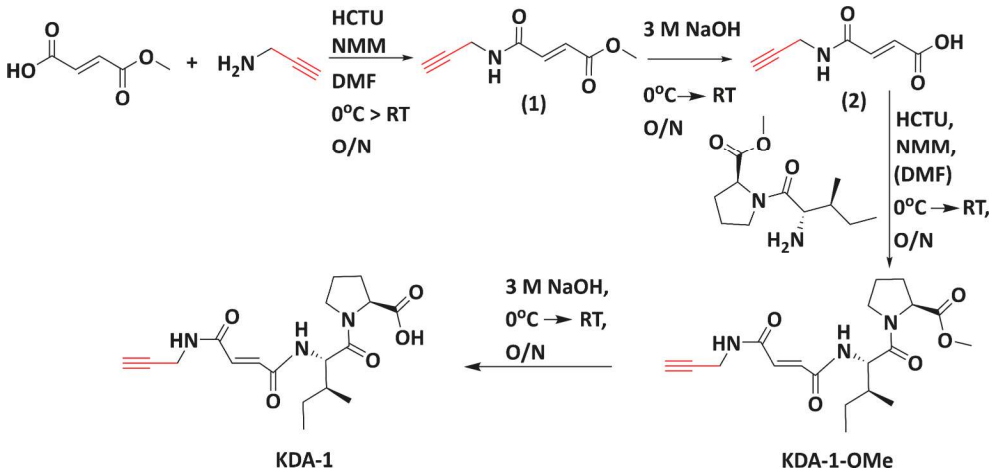


**Scheme 1.** Synthetic strategy utilized in the acquisition of a cell penetrable, clickable and tagless human cathepsin B probes, KDA-1-OMe, and its non-cell penetrable analogue, KDA-1.

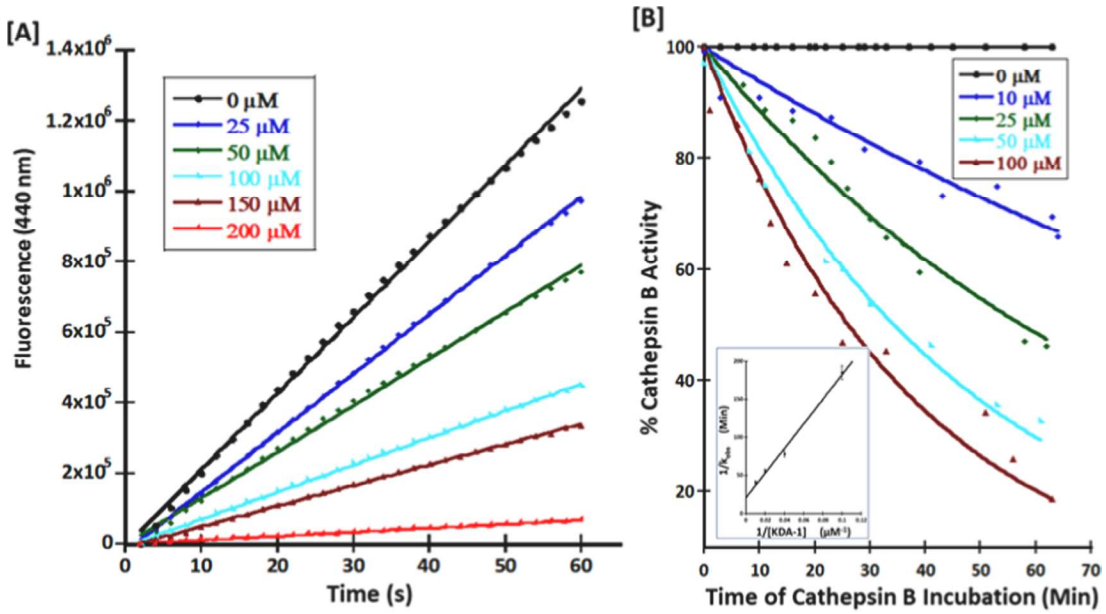


**Fig. 2.** Kinetic characterization of KDA-1-mediated inhibition of human liver cathepsin B enzyme. [A] Inhibition of human liver cathepsin B activity by KDA-1 probe in a dose dependent manner is demonstrated by monitoring the hydrolysis of Z-RR-AMC substrate ($K_m$ = 6.13 µM) at 440 nm. [B] Time-dependent nature of human liver cathepsin B inhibition; Incubation of appropriate concentrations of KDA-1 with cathepsin B under pseudo-first order condition (i.e. [KDA-1]≫[cathepsin B]) leads to a time-dependent loss of cathepsin B activity. Inset plot shows Kitz-Wilson analysis of the inhibitory data, yielding a $k_{inact}$ = 0.05 ± 0.01 $min^{-1}$ and $K_i$ = 76 ± 21 µM.

**Table 1**
Selectivity profile of cathepsin B probe, KDA-1 against closely-related cysteine cathepsin L and S.

| Enzyme | Second order Inactivation Rate Constant ($M^{-1}$ $min^{-1}$) |
|---|---|
| Human Cathepsin B | 653[a] |
| Human Cathepsin L | NI[b] |
| Human Cathepsin S | NI[b] |

[a] Calculated from parameters obtained using Kitz-Wilson analysis.
[b] No inhibition at 200 µM with 1.5 hr of reaction.

PAGE, and the gel scanned directly using Typhoon Scanner (ex.: 532 nm, em.: 580 nm). It is evident that KDA-1 can successfully label active cathepsin B enzyme (Fig. 4A). In control experiments, where cathepsin B was first fully inactivated using commercially available inhibitors (CA-074, selective toward cathepsin B and E64d, a pan-cathepsin inhibitor), and subsequently incubated with KDA-1 did not show any labeling (Fig. 4B, lane a and b); active cathepsin B alone when treated with 5-TAMARA-azide did not also show any labeling, as anticipated (Fig. 4B, lane c). These experiments demonstrate that KDA-1 is indeed capable of reporting on the 'activity' profile of human cathepsin B enzyme.

### *2.4. KDA-1-OMe probe is cell permeable and inhibits intracellular cathepsin B activity in live human MDA-MB-231 breast cancer cells*

For KDA-1-OMe probe to be effective for assessing the activity profiles of human cathepsin B in proteomes derived from a diverse cell types, it was important to demonstrate that the KDA-1-OMe probe was indeed cell penetrable, and was capable of labeling cellular cathepsin B activity in live cells. It was anticipated that the methyl ester of KDA-1-OMe would readily be cleaved by cellular esterases, rendering it ready for labeling. Methyl ester of a carboxylic acid compound is a well known

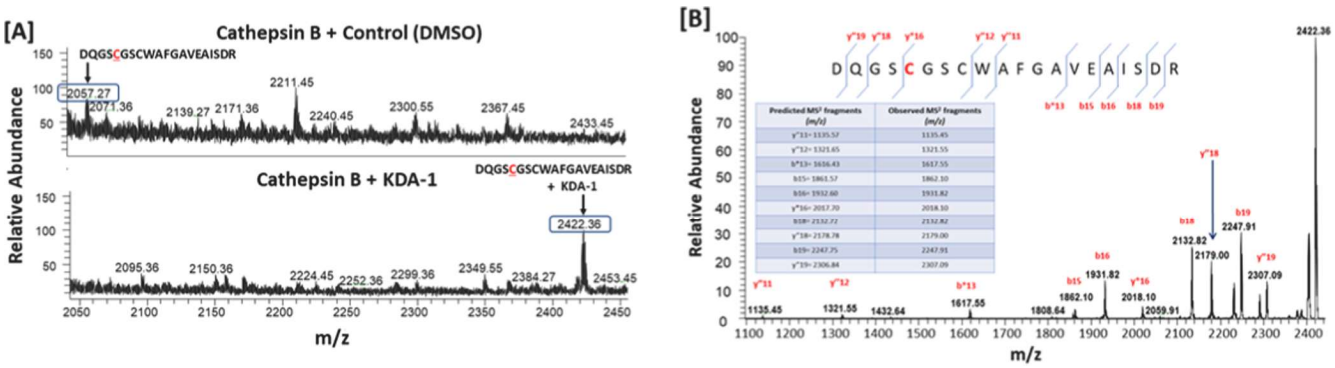


**Fig. 3.** Evidence of a covalent, irreversible, and active site-targeted nature of human cathepsin B inhibition by KDA-1 probe using mass spectrometry: **[A]** Mass spectrum represents active site Cys29-containing peptide from the tryptic digest of human cathepsin B, modified by KDA-1, with control (DMSO) **[B]** MS/MS spectrum of fragment 2422.36 Da confirms that the target residue of KDA-1 in cathepsin B is the catalytic Cys29 residue.

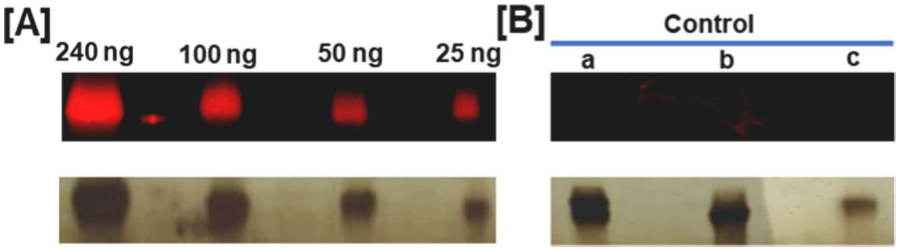


**Fig. 4.** Fluorescence Imaging of active human cathepsin B, labelled with, KDA-1. **[A]** Purified and activated human cathepsin B was incubated with KDA-1. After the reaction was quenched, labelled cathepsin B was clicked with 5-TAMRA-azide, resolved using SDS-PAGE, and detected using a Typhoon 9400 scanner (ex: 532 nm, em: 580 nm). **[B]** Control experiments: (i) Lanes a and b contain active human cathepsin B that was inactivated first with known cathepsin B inhibitor, CA-074, and pan cathepsin inhibitor, E64d, respectively, prior to incubation with KDA-1 probe, and click chemistry performed as noted (loaded 200 ng); (ii) Lane c was active cathepsin B alone, without any prior inactivation/labeling, treated with 5-TAMARA-azide using identical protocol (loaded 40 ng). Bottom panels are silver-stained images of the same gel.

strategy for probe delivery to the live cellular compartment.[41,42,44] For this experiment, triple negative human MDA-MB-231 breast cancer cell lines was chosen where cathepsin B expression is relatively high. Treatment of live MDA-MB-231 cells with KDA-1-OMe resulted in a dose-deependent loss of cellular cathepsin B activity, suggesting that the probe is indeed cell-penetrable and can function in living cells (Fig. 5).

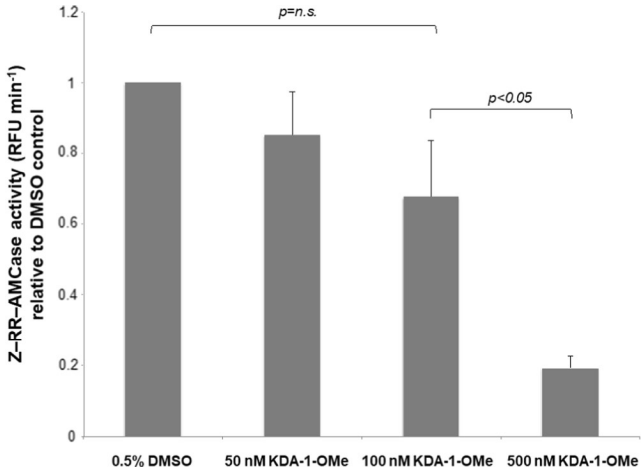


**Fig. 5.** KDA-1-OMe inhibits intracellular cathepsin B in MDA-MB-231 cells. Live MDA-MB–231 cells were treated (5 hrs) with 0.5% DMSO (solvent control) or various concentrations of KDA-1-OMe. After washing to remove any extracellular probe, cells were permeabilized with digitonin, and cathepsin B activity was measured using the fluorescence-based cathepsin B substrate Z-RR-AMC. The experiments were performed in triplicate and the results are presented as the mean (±s.d.) of the velocities of the change in fluorescence due to the release of free AMC in cells treated with KDA-1-OMe relative to the release in solvent control. The observed dose-dependent loss of cathepsin B activity indicates that KDA-1-OMe is membrane permeable and can inhibit cathepsin B in living cells.

### 2.5. *Functional validation of KDA-1-OMe probe labeling of cellular cathepsin B*

The involvement of human cathepsin B in highly invasive cancers is well-documented.[45–49] Since overabundant cathepsin B can promote tumor growth, we anticipated that its cellular inhibition by the cell-penetrable probe should reduce cell proliferation. Cell proliferation was thus assessed both in the presence of KDA-1-OMe probe, and compared with the vehicle control (Fig. 6[A]-[C]). A notable reduction in cell proliferation phenotype by KDP-1-OMe probe was observed, consistent with disrpution of cellular cathepsin B function in MDA-MB-231 cells. This observation was also supported by measuring cell viability using the MTT assay in 96-well format. A dose-dependent loss of cell viablity was observed, as expected (Fig. 6D), corroborating earlier findings that cathepsin B inhibition by small molecules is an attractive strategy for therapeutic anti-cancer drug development.[47,48]

### 2.6. *KDA-1 labels intracellular human cathepsin B in MDA-MB-231 and HEK293 cells*

Having demonstrated that KDA-1 was capable of labeling purified active human cathepsin B, we wanted to next assess its utility in labeling this enzyme at the proteome levels. In preliminary experiments, to investigate this we chose the proteome derived from MDA-MB-231 cells where cathepsin B expression is endogenously relatively high.[41,50] We also utlized proteome from transiently overexpressed hcathepsin B in HEK293 cell lines. Thus, freshly prepared proteomes were incubated with KDA-1 probe for 2 hrs. For detection of hcathepsin B in the proteomes post-labeling, click chemistry protocol was implemented using 5-TAMRA-Azide. The proteins were resolved using SDS-PAGE, and the

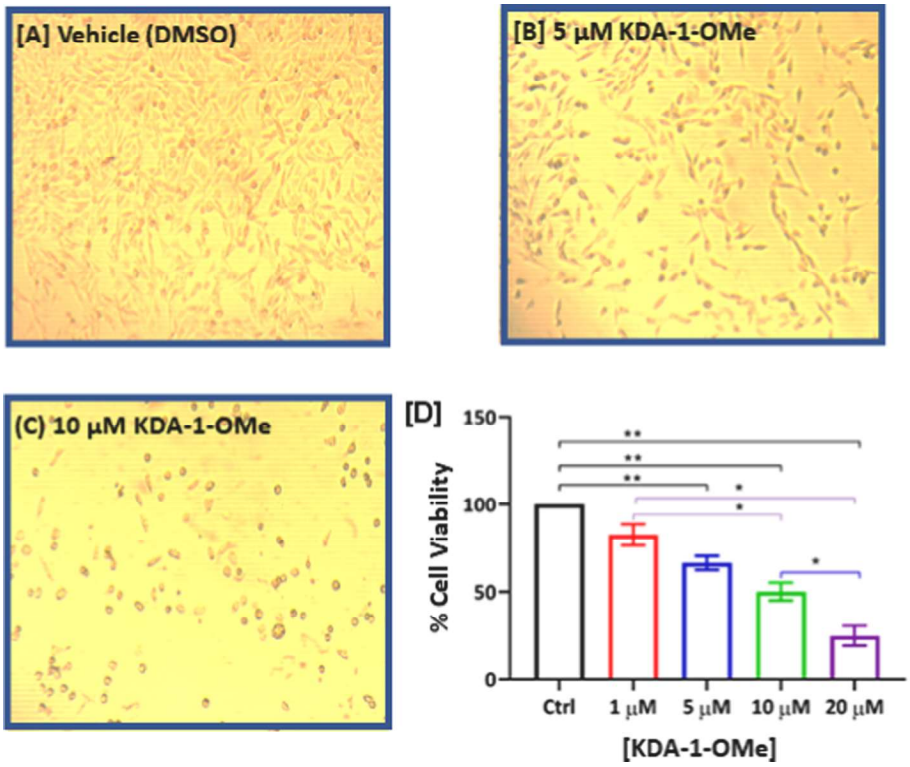


**Fig. 6.** [A-C] Anti-proliferative potential of cathepsin B probe, KDA-1-OMe, on MDA_MB-231 breast cancer cells that exogenously express high levels of cathepsin B. Cells were treated for 24hrs with vehicle control [A], and 5 and 10 µM of KDA-1-OMe, and imaged using an inverted phase contrast microscope. The experiments were perfomed in triplicates and representative images from one set are shown here [D] A concentration-dependent reduction in cell viability is observed upon 24hrs treatment with KDA-1-OMe probe, as anticipated from inhibition of cellular cathepsin B. ** $p < 0.01$, *$p < 0.05$.

gel scanned directly using Typhoon Scanner (ex.: 532 nm, em.: 580 nm). Although the proteomes contained thousands of proteins, KDA-1 was able to suceessfully label human cathepsin B (~6 kDa band) in both proteomes (Fig. 7). It should be noted that fully active cathepsin B is comprised of a light chain (~6 Kda) and a heavy chain (~25 kDa), joined by disulfide bridges.[51,52] The target residue of KDA-1, the active site Cys29 residue, lies in the light chain that is not detectable by exisitng antibodies, as also noted by Poreba et al..[29] We did not detect full length hcathepsin B in our experiments. While a few other nonspecific bands are obsevered in proteomes from both MDA-MB-231 (at ~25 kDa and 75 kDa) and HEK293 cells (between 25 kDa and 75 kDa), the utility of KDA-1 is promising in detection of cathepsin B activity. In future studies, we plan to optimize the labeling and click chemistry protocol conditions involving KDA-1-OMe probe so we can perform labeling on living cells and report on activity profiles of hcathepsin B enzyme from proteomes of both normal and diseased cells. Different chemical components of the click chemistry protocols have been shown to have markedly pronounced effects on click chemistry efficiency.[53]

## 3. Conclusions

In summary, we have developed a fumarate diamide-based clickable probe, KDA-1, that exhibits exclusive selectivity toward human cathepsin B enzyme; selectivity is an important criterion for small molecules, given how closely several cysteine dependent enzymes, including cathepsins, are related.[54] The mechanism of labeling is covalent, irreversible, and activity-dependent, as evident from steady-state enzymology experiments. Using mass spectrometric analysis, we demonstrate that the covalent target of this probe is the conserved Cys29 catalytic residue. That the developed KDA-1 probe is capable of labeling human cathepsin B in an activity-dependent manner with efficient post-labeling detection is also demonstrated. Using cell-permeable version of the probe (KDA-1-OMe), we show that this inhibitory probe can disrupt cellular cathepsin B function in triple negative human MDA-MB-231 breast cancer cells. Finally, we demonstrate that KDA-1 is capable of labeling human cathepsin B at the proteome levels in both MDA-MB-231 and hCathepsin B-overexpressing HEK293 cells. The key advantages of the KDA-1 probe are that it is small, selective, cell permeable and is devoid of bulky fluorophore/quencher moieties, thereby 'potentially' allowing efficient labeling to be performed in a natural cellular environment.[55,56] Further optimization of labeling and click chemistry protocols on living cells are planned in future studies for activity-based profiling of human cathepsin B enzyme utilizing the cell permeable, KDA-1-OMe probe. Further, we will perform a systematic SAR at S1′ position using a library of compounds that would exhibit a superior kinetic and labeling profile towards human cathepsin B enzyme. These studies taken together are anticipated to significantly augment our current understanding of cathepsin B biology in both normal and diseased states.

## 4. Experimental

### 4.1. Organic Synthesis

#### 4.1.1. General

The $^{1}H$ NMR and $^{13}C$ NMR spectra were recorded at 400 MHz (Brucker Inc.) using $CDCl_3$ or DMSO as the solvent. Chemical shifts ($\delta$) are reported in parts per million (ppm) and referenced to $CDCl_3$ (7.26 ppm for $^{1}H$ and 77.0 ppm for $^{13}C$), DMSO (2.50 ppm for $^{1}H$, $H_2O$ 3.33 ppm, and 39.50 ppm for $^{13}C$). The coupling constants ($J$) were reported in Hertz (Hz) and multiplicities are abbreviated as singlet (s), doublet (d), doublet of doublets (dd), triplet (t), triplet of doublets (td), and multiplet (m). The mass spectra were acquired on Matrix-Assisted Laser Desorption Ionization (MALDI)-Linear Ion Trap (LTQ) mass spectrometer (Thermo Scientific, Waltham, MA, USA). Monomethyl fumarate and propargylamine were purchased from AK scientific, Isobutyl chloroformate from ACROS organics and O-(1H-6-Chlorobenzotriazole-1-yl)-1,1,3,3-tetramethyluronium hexafluorophosphate (HCTU) was purchased from peptide international (Louisville, Kentucky, USA). All anhydrous solvents were purchased from Sigma-Aldrich (St. Louis, MO, USA). All other materials were purchased from Fisher Scientific Inc. (Pittsburgh, PA, USA) unless otherwise mentioned in the text.

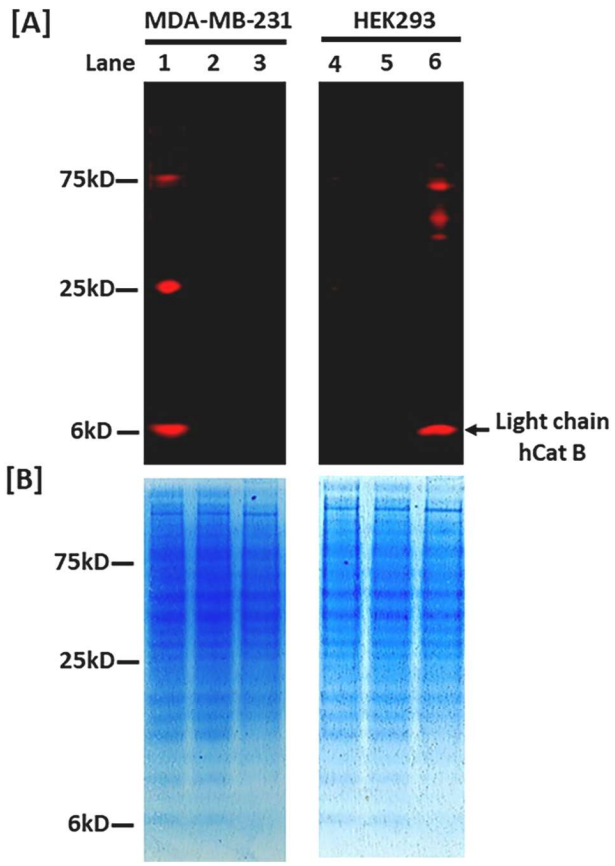


**Fig. 7.** Proteome-wide detection of human cathepsin B in human MDA-MB-231 breast cancer cells and HEK293 cells. Freshly prepared proteomes were labelled by KDA-1, followed by click chemistry protocol for detection using 5-TAMARA-azide. The resulting proteomes containing 15 μg proteins were resolved using SDS-PAGE. [A] Scanned SDS-PAGE gel (ex.: 532 nm, em.: 580 nm) from both sources of proteomes show the labeled hcathepsin B (~6 kDa light chain). Lanes 1 and 6: Cell lysate + KDA-1 + Click chemistry; Lanes 2 and 5 (Control): Cell lysate + Click chemistry; Lanes 3 and 4 (Control): Cell lysate alone [B] Coomassie stain of the gel, as used in [A], representing the entire proteome.

#### 4.1.2. Synthesis protocol

The synthesis of the clickable and tagless activity-based probe (cat-ABP), KDA-1 was achieved following the Scheme 1, as described below.

#### 4.1.3. Methyl (E)-4-oxo-4-(prop-2-yn-1-ylamino)but-2-enoate (1)

Monomethyl fumarate (500 mg, 1 eq, 3.8 mmol) was dissolved in small amount of anhydrous N,*N*-Dimethylformamide (DMF) under argon and cooled to 0 °C. To this was sequentially added *N*-methyl morpholine (NMM; 1.2 mL, 3 eq, 11 mmol), HCTU (2.36 g, 1.5 eq, 5.7 mmole), andpropargylamine (270 uL, 1.1 eq, 4.2 mmole). The reaction mixture was stirredovernight and allowed to warm up to room temperature. The reaction was quenched by pouring over ethylacetate and washed with 3x volumes of brine. The organic layer was dried over anhydrous sodium sulfate and the resulting crude was dried over high vacuum overnight. Yield: 95 %. From total product, 15 mg of compound was purified by HPLC for analysis and the fractions were lyophilized to get the desired product as white powder. $^{1}$H NMR (400 MHz, DMSO) $\delta$ ppm: 3.12–3.13 (t, $J$ = 2.45 Hz, 1H), 3.66 (s, 1H), 3.91–3.93 (q/m, $J$ = 2.51 Hz, $J$ = 2.98 Hz, $J$ = 2.47 Hz, 2H), 6.53–6.57 (d, $J$ = 15.62 Hz, 1H), 6.91–6.95 (d, $J$ = 15.50 Hz, 1H), 8.91–8.94 (t, $J$ = 5.30 Hz). $^{13}$C NMR (400 MHz, DMSO) $\delta$ ppm: 28.19, 52.58, 73.59, 80.27, 128.68, 136.79, 162.51, 165.39.

#### 4.1.4. (E)-4-oxo-4-(prop-2-yn-1-ylamino)but-2-enoic acid (2)

The compound (1) was dissolved in minimum amount of methanol. The solution was cooled at 0 °C and 3 M of NaOH was added. The reaction was run overnight and allowed to warm up to room temperature. The reaction was quenched by pouring over ethylacetate and washed with 3x volumes of water. The water layer was acidified using HCl 5 M (bring around pH = 1) and extracted with ethylacetate. The organic layer was dried over anhydrous sodium sulfate and removed *in vacuo*. Yield: 70 %. 15 mg of compound was purified by HPLC for analysis and the fractions were lyophilized to get the desired product as white powder. $^{1}$H NMR (400 MHz, DMSO) $\delta$ ppm: 3.11–3.12 (t, $J$ = 2.50 Hz, 1H), 5.84–6.11 (q, 2H), 6.46–6.49 (d, $J$ = 15.34 Hz, 1H), 6.81–6.85 (d, $J$ = 15.34 Hz, 1H), 8.85–8.88 (t, $J$ = 5.25 Hz, 1H), 12.84 (s, 1H). $^{13}$C NMR (400 MHz, DMSO) $\delta$ ppm: 73.89, 80.62, 130.34, 136.38, 163.03, 166.43.

#### 4.1.5. Ile-Pro-OMe

This compound was synthesized using the protocol outlined in the supporting information (Scheme S1).

#### 4.1.6. KDA-1-OMe

Compound (**2**) (632 mg, 2 eq, 4.1 mmol) was dissolved in small amount of anhydrous N,*N*-Dimethylformamide (DMF) under argon and cooled to 0 °C. To this was sequentially added NMM (1.1 mL, 5 eq, 10 mmol), HCTU (2.48 g, 3 eq, 6 mmole), and Ile-Pro-OMe (500 mg, 1 eq, 2.0 mmole). The reaction mixture that slowly warmed up to room temperature was stirred overnight. The reaction was quenched by pouring over ethyl acetate and washed with 3x volumes of brine. The organic layer was collected over anhydrous sodium sulfate and, subsequently, removed *in vacuo*. The crude product was purified using reverse phase HPLC and the fractions were lyophilized to get the desired product as powder (Yield: 76 %). $^{1}$H NMR (400 MHz, DMSO) $\delta$ ppm 0.88 (t, 3H), 0.91 (d, 3H, 6.75 Hz), 1.1 (m, 1H), 1.5 (m, 1H), 1.85–1.75 (m, 2H), 1.9–1.95 (m, 2H), 2.1–2.2 (m, 1H), 3.2 (t, 1H), 3.6–3.64 (m, 3H), 3.8–3.9 (m, 1H), 3.95–3.97 (q, 2H), 4.3–4.3 (q, 1H), 4.4–4.4 (t, 1H), 6.78–6.82 (d, 1H, 14.92 Hz), 6.97–7.0 (d, 1H, 15.23 Hz), 8.7–8.7 (d, 1H, 8.3 Hz), 8.8–8.8 (t, 1H). $^{13}$C NMR (400 MHz, DMSO) $\delta$ ppm: 10.58, 14.54, 24.22, 24.52, 28.04, 28.68, 36.05, 46.94, 51.69, 54.63, 58.42, 73.37, 80.54, 132.35, 132.86, 163.37, 169.86, 172.17, 171.17 HRMS (*m/z*): $[M+Na]^+$ for molecular formula $C_{19}H_{27}N_3O_5Na$: calculated 400.1848; found 400.1846.

#### 4.1.7. KDA-1

3 M NaOH solution was dropwise added to an ice-cold solution of KDA-1-OMe in methanol. The reaction mixture was stirred overnight and allowed to warm up to room temperature. The reaction was quenched by pouring over ethylacetate and washed with 3x volumes of distilled water. The water layer was collected and acidified using 5 M HCl to pH 1, which was further extracted with ethyl acetate. The organic layer was collected and dried over anhydrous sodium sulfate. The solvent was evaporated *in vacuo* and the resulting crude was purified using reverse phase HPLC to obtain the desired product as white powder after lyophilization. (Yield 65%). $^{1}$H NMR (500 MHz, DMSO) $\delta$ ppm 0.82 (t, 3H), 0.88 (d, 3H, 6.75 Hz), 1.10 (m, 1H), 1.48 (m, 1H), 1.70 (m, 1H), 1.82 (m, 1H), 1.91 (m, 2H), 2.17 (m, 1H), 3.24 (m, 1H), 3.4 (s, 1H), 3.58 (m, 1H), 3.61 (s, 3H), 3.79 (m, 1H), 4.04 (t, 1H), 4.31 (m, 1H), 6.92 (d, 1H), 7.43–7.45 (d, 1H),7.90 (s, 1H), 8.04–8.05 (d, 1H), 13.86 (bs, 1H). $^{13}$C NMR (400 MHz, DMSO) $\delta$ ppm: 12.70, 17.0, 18.0, 41.50, 53.10, 73.31, 83.18, 109.65, 119.02, 124.39, 127.16, 127.84, 132.35, 158.11, 158.44, 163.35, 169.75, 173.17. HRMS (*m/z*): $[M+Na]^+$ for molecular formula $C_{18}H_{25}N_3O_5Na$: calculated 386.1691; found 386.1692.

### 4.2. Inhibitory enzymology

#### 4.2.1. Determination of kinetic inactivation parameters of KDA-1 against human cathepsin B

The inactivation reaction of hcathepsin B (net 177 nM, Enzo Life

Sciences Inc.) by appropriate concentrations (0, 10 μM, 25 μM, 50 μM, 100 μM) of inhibitor was performed under pseudo-first-order condition ([I]≫[E]) in a 0.5 mL tube maintained at 30 °C in a temperature-controlled bath. hCathepsin B was first activated for 10 min in sodium acetate buffer (100 mM, pH 5.5) containing 8 mM DTT and 4 mM $Na_2EDTA$. The inactivation reaction was initiated by the addition of a fixed concentration of KDA-1 where DMSO concentration was maintained at 5%. After suitable time intervals, an aliquot of 10 μL of incubation mixture was withdrawn and added to an assay mixture (net assay volume 200 μL) that contained 30 μM of Z-RR-AMC ($K_m$ = 6.13 μM) substrate at 30 °C. A progress curve was recorded (excitation: 365 nm; emission: 440 nm) and the enzyme activity was determined by measuring the initial rates of substrate turnover. The postulated kinetic inactivation mechanism involved a two-step enzyme inactivation process, a reversible initial inhibitory binding event followed by the covalent modification of the enzyme:

$$E + I \overset{K_i}{\rightleftharpoons} E.I \overset{k_{inact}}{\rightarrow} E - I$$

The initial rates (v) thus obtained were plotted against the time of enzyme inactivation reaction (t). The plot was then fitted to $v = v_0 * e^{-k_{obs} * t}$ to obtain $k_{obs}$, the pseudofirst order rate constant of enzyme inactivation (KaleidaGraph version 4.5.4 software; Script: m1*exp (-m2*m0); m1 = 1; m2 = 1). The $k_{obs}$ thus obtained at various concentration of probe KDA-1 was fitted to Kitz-Wilson equation ($\frac{1}{k_{obs}} = \left(\frac{K_i}{k_{inact}}\right) * \frac{1}{[I]} + \frac{1}{k_{inact}}$) using KaleidaGraph version 4.5.4 software [Script: ((m1/m2) *m0)+(1/m2); m1 = 1; m2 = 1], as previously described.[57] This resulted in obtaining the thermodynamic inhibition constant ($K_i$) and the first-order inactivation rate constant ($k_{inact}$) for the inhibition reaction involving KDA-1 and human cathepsin B.

#### 4.2.2. Determination of selectivity of KDA-1 against human cathepsin S and L

For assaying cathepsin S activity, a previously published protocol was utilized.[58] The cathepsin L inhibition assay procedure was also adopted from an earlier published protocol.[56]

### 4.3. Mass spectrometry

The samples of inhibited KDA-1/cathepsin B complex alongside cathepsin B (control) were analyzed using Matrix-Assisted Laser Desorption Ionization (MALDI)-Linear Ion Trap (LTQ) mass spectrometer (Thermo Scientific, Waltham, MA, USA) utilizing nitrogen laser (337 nm) firing at 60 Hz. For MS analysis inhibited KDA-1/cathepsin B complex and cathepsin B (control) samples were resolved on SDS-PAGE; the band was excised, and in-gel digestion was performed using trypsin (Promega Inc., USA). The digested samples were further concentrated and purified using ZipTip C18 (Merck Millipore, IRL) followed by elution of the retained peptides directly on MALDI probe. Mass spectra of samples were typically obtained using 300 scans and processed with Xcalibur (2.0.7 SP1) software.

### 4.4. hCathepsin B labeling experiments

Human liver cathepsin B (6 μL, 2.56 μg) was first activated for 10 min at 30 °C in 13.5 μL of sodium acetate buffer (100 mM, pH 5.5) containing 8 mM DTT and 4 mM $Na_2EDTA$. The inactivation reaction was initiated by the addition 1.5 μL (2.59 mM net) of KDA-1 probe for 1 h. Next we added 10 μL of HPLC grade water, 2 μL of $CuSO_4$ (4.76 mM net), 2 μL of sodium ascorbic acid (4.76 mM net), 2 μL of THPTA (4.76 mM net) and, finally 1 μL of TAMRA solution (95 μM net). The reaction was allowed to procced for 2 h at 37 °C. Reaction was quenched by addition of 3 μL of 1X Laemmli buffer. Different amount of TAMRA-KDA-1-cathepsin B complex were resolved using SDS-PAGE (12%) and the gel was washed with distilled water for 1 h. The gel was then scanned on Typhoon 9400 scanner (ex: 532 nm, em: 580 nm) and analyzed using ImageJ software.[59] For assessing the loaded protein amount, the gel was stained using ThermoFisher Silver Staining kits, as recommended by the manufacturer. In control experiments a and b, the active human cathepsin B (240 ng loaded) were pre-incubated with commercially available cathepsin B inhibitor, CA074 (0.6 mM net), and pan-cathepsin inhibitor E64d (0.6 mM net) respectively for 1 h. After this was added KDA-1 (0.8 mM net) probe, and the resulting reaction mixture was further incubated for 30 min. In control experiment c, pure and active human cathepsin B (85 ng loaded) was directly subjected to identical click chemistry and detection protocol without any inactivation reaction. The control protein samples were then resolved on SDS-PAGE and click chemistry and subsequent detection experiments were done under identical conditions.

### 4.5. Cell biology studies

#### 4.5.1. General

HEK293 and MDA-MB231 cells were purchased from ATCC and maintained in DMEM media (Fisher Scientific, Cat # 11995065,) with 10% Fetal Bovine Serum (Fisher Scientific, Cat # FB12999102), 1% Penicillin-Streptomycin (Gibco Cat # 15140–122) and 1% non-essential amino acids (Gibco Cat # 11140–050). For cathepsin B overexpression in HEK293 cells: hCathepsin B plasmid in the form of bacterial stab was obtained from Addgene (plasmid # 11,249 - a gift from Hyeryun Choe; http://n2t.net/addgene:11249; RRID: Addgene_11249).[60] Plasmid DNA isolation was done using a midiprep kit from Life Technologies (Cat # K210004). For transfection, Lipofectamine (Cat# L3000001, Fisher Scientific Inc.) was used and protein estimation was conducted using a BCA protein assay kit from Pierce (Cat # PI23225). NuPAGE 4–12% Bis-Tris mini gels (NP0335box) with MES buffer (NP0002), used for gel electrophoresis, were obtained from Life Technologies Corp. Unless otherwise specified all other chemicals were purchased from Fisher Scientific.

#### 4.5.2. Transient overexpression of hCathepsin B in HEK293 cells

For transient overexpression of human cathepsin B in HEK293 cells, the following protocol was adopted: A toothpick stab of hCathepsin B (Addgene Inc.) containing stock bacteria was grown in 10 mL sterile LB media containing 50 μg/ml ampicillin on a 37 °C shaker at 250 rpm for 6 h. From that culture, 100 μL of bacteria was transferred to 100 mL of LB media containing ampicillin and the culture was allowed to grow for 16 hrs on a shaker at 250 rpm and at 37 °C. Plasmid DNA was isolated using the kit specified above and DNA concentration was measured using a Nanodrop. Transient Transfection of HEK293 cells and preparation of cell lysate: For HEK-293 cells, transient transfection of hCathepsin B was performed following the kit instructions as specified by the manufacturer.

#### 4.5.3. Assessment of cellular permeability

Repnick's Method was used. MDA MB–231 cells were plated at 10–15 × $10^4$ /well in complete medium cells in black transparent bottom 96–well plates. The following day, fresh media was added containing one of the following: 0.5% DMSO; 50, 100, 250, or 500 nM KDA-1-Me. After 5 h, soluble extracellular inhibitors were removed by aspirating the media and washing the cells with phosphate–buffered saline. Next, a cellular lysate was made by solubilizing the plasma membrane and intracellular membranes by adding 50 μL of 200 μg/mL digitonin in acetate buffer (50 mM sodium acetate pH 5.6, 150 mM NaCl, 0.5 mM EDTA) to the wells containing the cells and incubating on ice for 10–15 min. We next added 50 μL of the Cathepsin B fluorogenic substrate Z-RR-AMC (Benzyloxycarbonyl-arginyl-arginyl-7-amido-4-methyl coumarin) in sodium acetate buffer directly to the lysates in the wells for a final concentration of 30 μM Z–RR–AMC and 5 mM DTT. We quantified the release of free AMC in each well using a SpectraMax M4 in kinetic mode at 380 nm excitation and 460 nm emission. The reaction was run for 60 min at 25 °C with readings recorded every 30 s and the velocity of the

reaction was calculated using Excel. The experiments were repeated in 3 independent trials and each trial represented a technical replicate of two. Because of a small variability in amount of substrate or the number of cells in different trials, we normalized the slopes of the lines produced in each trial relative to the DMSO control from that trial. A one-way ANOVA was conducted to compare the effect of KDA–1–OMe on intracellular cathepsin B. At 500 nM KDA–1–Me there was a significant inhibition of Z-RR-AMC cleavage at the $p < 0.05$ level when compared to DMSO control and 50 and 100 nM KDA–1–OMe. Because these data were proportional (percentages), significance was assessed by first transforming the percentage data using an arcsine transformation followed by a t Test with Bonferroni correction.

#### 4.5.4. Cell proliferation and cell viability studies

The triple negative human MDA-MB-231 breast cancer cells were grown in 75 $cm^2$ tissue culture flasks in culture medium [DMEM (Millipore Sigma, USA) medium, supplemented with 10% FBS (Atlanta Biologicals, FBS – Premium, GA), 0.1% penicillin/streptomycin (Gibco, ThermoFisher Scientific, USA), 0.1% nonessential amino acid (Gibco, ThermoFisher Scientific, USA)] and maintained at 37 °C under 5% $CO_2$ environment. The final concentration of DMSO in all cell culture medium was maintained at 0.3%. For the cell proliferation assay, cells were plated into 6-well plates at a density of $1 \times 10^6$ cell/well in 2 mL of culture media and were grown for 24 h in the incubator. Subsequently, the cells were treated with KDA-1-OMe probe for 24 h at 5 μM, and 10 μM concentrations, with DMSO (0.3%) as the negative control (Fig. 6 [A-C]). The cells were observed using inverted phase contrast microscope (JENCO Inc., USA) and images were captured using the digital camera (OMAX Inc., A3518043).

For the cell viability assay, cells were plated into 96 well plates at a density of 5000 cell/well in 200 μL of culture media and were grown for 24 h. They were then treated with KDA-1-OMe probe (1 μM, 5 μM, 10 μM, 20 μM, and DMSO as negative control) for 24 h. The medium was then replaced with RPMI 1640 (Gibco, ThermoFisher Scientific, USA) without phenol red, containing 5 mg/mL MTT (Tetrarazoliumbromid, Acros Organics, USA) and cells were incubated for 4 h. The medium was removed, and the precipitate was dissolved with 100 μL of DMSO, followed by detection of absorption at 560 nm; the background was subtracted using empty wells. The data was plotted using Graphpad Prism version 8.2.1 (Fig. 6D). Subsequently, we generated a dose–response curve and fitted the data to determine the the $EC_{50}$ value against MDA-MB-231 cells (23 ± 1 μM; See SI Figure S1).

#### 4.5.5. Proteome-wide labeling and identification of hCathepsin B enzyme in human MDA-MB-231 breast cancer cells and cathepsin B overexpressing HEK293 cells

MDA-MB231 cells were maintained in DMEM media in the composition as suggested by ATCC. At about 90% confluency, cells were lysed under non-denaturing condition using an ice-cold buffer containing 20 mM Tris-base, 200 mM NaCl, 1% Triton (pH 7.4) with protease and phosphatase inhibitors, and protein concentration was estimated by BSA protein assay kit. For preparation of Cathepsin B-overexpressing HEK293 cell lysate, the following protocol was utilized: 48 h post transfection, media was aspirated, cells were washed with PBS and lysed under non-denaturing condition, as described for MDA-MB-231 cells. Cells were scraped off, centrifuged and the supernatant was used to estimate protein concentration.

For labeling and detection of endogenously active hCathepsin B using click chemistry, the following protocol was utilized: 4.8 μL (3.1 μg/μL) of freshly prepared lysate from HEK293 and 10.6 μL (1.4 μg/μL) from MDA-MB-231 were incubated separately with 1.5 μL (2.59 mM net) of KDA-1 probe for two hours. To this was added in sequence 6.2 μL and 0.4 μL of HPLC grade water respectively, 2 μL of CuSO4 (4.76 mM net), 2 μL of sodium ascorbic acid (4.76 mM net), 2 μL of THPTA (4.76 mM net) and, finally 1 μL of 5-TAMRA-azide solution (95 μM net). The reaction was run for three hours at 25 °C and was subsequently quenched by the addition of 5 μL of Laemmli buffer 1×. The resulting proteomes (15 μg) were then resolved on a 12% SDS-PAGE gel with MES buffer at 200 V for 35 min. The gel was washed thoroughly in distilled water for 8 h (2x) and then scanned on Typhoon 9400 scanner using an excitation filter at 532 nm and emission at 580 nm. Image analysis was performed using the ImageJ software.[59] The scanned gel was then stained using Coomassie to observe the resolved proteins from the entire proteome.

## Declaration of Competing Interest

The authors declare that they have no known competing financial interests or personal relationships that could have appeared to influence the work reported in this paper.

## Acknowledgement

This work was supported by the National Science Foundation (NSF) under the Grant Number 1709711 to S.K.P.; K.R.F. thanks PSC–CUNY (Awards # 61414-00 49 and 62333-00 50). Authors wish to also thank Dr. Barney Yoo (Hunter College Mass Spectrometry Facility, NY, NY) for his help with HRMS of KDA-1 and KDA-1-OMe compounds.

## Appendix A. Supplementary material

Supplementary data to this article can be found online at https://doi.org/10.1016/j.bioorg.2021.105463.

## References

[1] M. Bogyo, Introduction to the special issue on proteases and proteolysis in health and disease, FEBS J. 284 (10) (2017) 1392–1393.
[2] B. Turk, S.A. Turk du, V. Turk, Protease signalling: the cutting edge, EMBO J. 31 (7) (2012) 1630–1643.
[3] V. Turk, V. Stoka, O. Vasiljeva, M. Renko, T. Sun, B. Turk, D. Turk, Cysteine cathepsins: from structure, function and regulation to new frontiers, BBA 1824 (1) (2012) 68–88.
[4] N. Aggarwal, B.F. Sloane, Cathepsin B: multiple roles in cancer, Proteom. Clin. Appl. 8 (5–6) (2014) 427–437.
[5] J. Reiser, B. Adair, T. Reinheckel, Specialized roles for cysteine cathepsins in health and disease, J. Clin. Investig. 120 (10) (2010) 3421–3431.
[6] N. Katunuma, Posttranslational processing and modification of cathepsins and cystatins, J. Signal Transd. 2010 (2010) 1–8.
[7] P.C. Almeida, I.L. Nantes, J.R. Chagas, Cláudia.C.A. Rizzi, A. Faljoni-Alario, E. Carmona, L. Juliano, H.B. Nader, I.L.S. Tersariol, Cathepsin B activity regulation. Heparin-like glycosaminogylcans protect human cathepsin B from alkaline pH-induced inactivation, J. Biol. Chem. 276 (2) (2001) 944–951.
[8] A.A. Aghdassi, D.S. John, M. Sendler, F.U. Weiss, T. Reinheckel, J. Mayerle, M. M. Lerch, Cathepsin D regulates cathepsin B activation and disease severity predominantly in inflammatory cells during experimental pancreatitis, J. Biol. Chem. 293 (3) (2018) 1018–1029.
[9] C. Paquet, A.-T. Sané, M. Beauchemin, R. Bertrand, Caspase- and mitochondrial dysfunction-dependent mechanisms of lysosomal leakage and cathepsin B activation in DNA damage-induced apoptosis, Leukemia: Off. J. Leukemia Soc. Am., Leukemia Res. Fund U.K. 19 (5) (2005) 784–791.
[10] M.A. Nouh, M.M. Mohamed, M. El-Shinawi, M.A. Shaalan, D. Cavallo-Medved, H. M. Khaled, B.F. Sloane, Cathepsin B: a potential prognostic marker for inflammatory breast cancer, J. Transl. Med. 9 (2011) 1.
[11] E.S. Baskin-Bey, A. Canbay, S.F. Bronk, N. Werneburg, M.E. Guicciardi, S. L. Nyberg, G.J. Gores, Cathepsin B inactivation attenuates hepatocyte apoptosis and liver damage in steatotic livers after cold ischemia-warm reperfusion injury, Am. J. Physiol. Gastrointest. Liver Physiol. 288 (2) (2005) G396–G402.
[12] R. Muniyappa, J.R. Sowers, Glycogen synthase kinase-3beta and cathepsin B in diabetic endothelial progenitor cell dysfunction: an old player finds a new partner, Diabetes 63 (4) (2014) 1194–1197.
[13] W. Halangk, M.M. Lerch, B. Brandt-Nedelev, W. Roth, M. Ruthenbuerger, T. Reinheckel, W. Domschke, H. Lippert, C. Peters, J. Deussing, Role of cathepsin B in intracellular trypsinogen activation and the onset of acute pancreatitis, J. Clin. Investig. 106 (6) (2000) 773–781.
[14] B. Turk, Targeting proteases: successes, failures and future prospects, Nat. Rev. Drug Discovery 5 (9) (2006) 785–799.
[15] L.M. Greenbaum, A. Hirshkowitz, I. Shoichet, The activation of trypsinogen by cathepsin B, J. Biol. Chem. 234 (1959) 2885–2890.
[16] C. Figarella, B. Miszczuk-Jamska, A.J. Barrett, Possible lysosomal activation of pancreatic zymogens. Activation of both human trypsinogens by cathepsin B and spontaneous acid. Activation of human trypsinogen 1, Bio. Chem. Hoppe-Seyler 369 (Suppl) (1988) 293–298.

[17] T. Wartmann, J. Mayerle, T. Kähne, M. Sahin–Tóth, M. Ruthenbürger, R. Matthias, A. Kruse, T. Reinheckel, C. Peters, F.U. Weiss, M. Sendler, H. Lippert, H. Schulz, A. Aghdassi, A. Dummer, S. Teller, W. Halangk, M.M. Lerch, Cathepsin L inactivates human trypsinogen, whereas cathepsin L-deletion reduces the severity of pancreatitis in mice, Gastroenterology 138 (2) (2010) 726–737.
[18] D.M. Klein, K.M. Felsenstein, D.E. Brenneman, Cathepsins B and L differentially regulate amyloid precursor protein processing, J. Pharmacol. Exp. Therap. 328 (3) (2009) 813–821.
[19] S. Cermak, M. Kosicek, A. Mladenovic-Djordjevic, K. Smiljanic, S. Kanazir, S. Hecimovic, M.K. Lakshmana, Loss of cathepsin B and L leads to lysosomal dysfunction, NPC-Like cholesterol sequestration and accumulation of the key Alzheimer's proteins, PLoS ONE 11 (11) (2016) e0167428.
[20] G.M. Orlowski, J.D. Colbert, S. Sharma, M. Bogyo, S.A. Robertson, K.L. Rock, Multiple cathepsins promote pro-IL-1β synthesis and NLRP3-mediated IL-1β activation, J. Immunol. 195 (4) (2015) 1685–1697.
[21] X.W. Cheng, G.-P. Shi, M. Kuzuya, T. Sasaki, K. Okumura, T. Murohara, Role for cysteine protease cathepsins in heart disease: focus on biology and mechanisms with clinical implication, Circulation 125 (12) (2012) 1551–1562.
[22] Q. Tang, J. Cai, D. Shen, Z. Bian, L. Yan, Y.X. Wang, J. Lan, G.Q. Zhuang, W.Z. Ma, W. Wang, Lysosomal cysteine peptidase cathepsin L protects against cardiac hypertrophy through blocking AKT/GSK3beta signaling, J. Mol. Med. (Berl) 87 (3) (2009) 249–260.
[23] C.-L. Liu, J. Guo, X. Zhang, G.K. Sukhova, P. Libby, G.-P. Shi, Cysteine protease cathepsins in cardiovascular disease: from basic research to clinical trials, Nat. Rev. Cardiol. 15 (6) (2018) 351–370.
[24] B.F. Cravatt, A.T. Wright, J.W. Kozarich, Activity-based protein profiling: from enzyme chemistry to proteomic chemistry, Annu. Rev. Biochem. 77 (2008) 383–414.
[25] S. Kumar, B. Zhou, F. Liang, W.-Q. Wang, Z. Huang, Z.-Y. Zhang, Activity-based probes for protein tyrosine phosphatases, PNAS 101 (21) (2004) 7943–7948.
[26] M. Fonovic, M. Bogyo, Activity based probes for proteases: applications to biomarker discovery, molecular imaging and drug screening, Curr. Pharm. Des. 13 (3) (2007) 253–261.
[27] R.M. Garbaccio, E.R. Parmee, The impact of chemical probes in drug discovery: a pharmaceutical industry perspective, Cell Chem. Biol. 23 (1) (2016) 10–17.
[28] V.V. Nemmara, P.R. Thompson, Development of activity-based proteomic probes for protein citrullination, Curr. Top. Microbiol. Immunol. 420 (2019) 233–251.
[29] M. Poreba, K. Groborz, M. Vizovisek, M. Maruggi, D. Turk, B. Turk, G. Powis, M. Drag, G.S. Salvesen, Fluorescent probes towards selective cathepsin B detection and visualization in cancer cells and patient samples, Chem. Sci. 10 (36) (2019) 8461–8477.
[30] M.R. Pratt, M.D. Sekedat, K.P. Chiang, T.W. Muir, Direct measurement of cathepsin B activity in the cytosol of apoptotic cells by an activity-based probe, Chem. Biol. 16 (9) (2009) 1001–1012.
[31] H.C. Hang, J. Loureiro, E. Spooner, A.W.M. van der Velden, Y.-M. Kim, A. M. Pollington, R. Maehr, M.N. Starnbach, H.L. Ploegh, Mechanism-based probe for the analysis of cathepsin cysteine proteases in living cells, ACS Chem. Biol. 1 (11) (2006) 713–723.
[32] G. Blum, S.R. Mullins, K. Keren, M. Fonovič, C. Jedeszko, M.J. Rice, B.F. Sloane, M. Bogyo, Dynamic imaging of protease activity with fluorescently quenched activity-based probes, Nat. Chem. Biol. 1 (4) (2005) 203–209.
[33] M.E. Roth-Konforti, C.R. Bauer, D. Shabat, Unprecedented sensitivity in a probe for monitoring cathepsin B: chemiluminescence microscopy cell-imaging of a natively expressed enzyme, Angew. Chem. 56 (49) (2017) 15633–15638.
[34] M.A. Chowdhury, I.A. Moya, S. Bhilocha, C.C. McMillan, B.G. Vigliarolo, I. Zehbe, C.P. Phenix, Prodrug-inspired probes selective to cathepsin B over other cysteine cathepsins, J. Med. Chem. 57 (14) (2014) 6092–6104.
[35] G. Blum, G. von Degenfeld, M.J. Merchant, H.M. Blau, M. Bogyo, Noninvasive optical imaging of cysteine protease activity using fluorescently quenched activity-based probes, Nat. Chem. Biol. 3 (10) (2007) 668–677.
[36] U. Machon, C. Büchold, M. Stempka, T. Schirmeister, C. Gelhaus, M. Leippe, J. Gut, P.J. Rosenthal, C. Kisker, M. Leyh, C. Schmuck, On-bead screening of a combinatorial fumaric acid derived peptide library yields antiplasmodial cysteine protease inhibitors with unusual peptide sequences, J. Med. Chem. 52 (18) (2009) 5662–5672.
[37] A. Breuning, B. Degel, F. Schulz, C. Büchold, M. Stempka, U. Machon, S. Heppner, C. Gelhaus, M. Leippe, M. Leyh, C. Kisker, J. Rath, A. Stich, J. Gut, P.J. Rosenthal, C. Schmuck, T. Schirmeister, Michael acceptor based antiplasmodial and antitrypanosomal cysteine protease inhibitors with unusual amino acids, J. Med. Chem. 53 (5) (2010) 1951–1963.
[38] J. Schmitz, E. Gilberg, R. Löser, J. Bajorath, U. Bartz, M. Gütschow, Cathepsin B: active site mapping with peptidic substrates and inhibitors, Bioorg. Med. Chem. 27 (1) (2019) 1–15.
[39] A. Yamamoto, K. Tomoo, T. Hara, M. Murata, K. Kitamura, T. Ishida, Substrate specificity of bovine cathepsin B and its inhibition by CA074, based on crystal structure refinement of the complex, J. Biochem. 127 (4) (2000) 635–643.
[40] D. Turk, M. Podobnik, T. Popovic, N. Katunuma, W. Bode, R. Huber, V. Turk, Crystal structure of cathepsin B inhibited with CA030 at 2.0-A resolution: a basis for the design of specific epoxysuccinyl inhibitors, Biochemistry 34 (14) (1995) 4791–4797.
[41] O. Ishibashi, Y. Mori, T. Kurokawa, M. Kumegawa, Breast cancer cells express cathepsins B and L but not cathepsins K or H, Cancer Biochem. Biophys. 17 (1–2) (1999) 69–78.
[42] M. Montaser, G. Lalmanach, L. Mach, CA-074, but not its methyl ester CA-074Me, is a selective inhibitor of cathepsin B within living cells, Biol. Chem. 383 (7–8) (2002) 1305–1308.
[43] R. Kitz, I.B. Wilson, Esters of methanesulfonic acid as irreversible inhibitors of acetylcholinesterase, J. Biol. Chem. 237 (10) (1962) 3245–3249.
[44] E. Krepela, J. Vicar, M. Cernoch, Cathepsin B in human breast tumor tissue and cancer cells, Neoplasma 36 (1) (1989) 41–52.
[45] C.S. Gondi, J.S. Rao, Cathepsin B as a cancer target, Exp. Opin. Therap. Targets 17 (3) (2013) 281–291.
[46] S.A. Rempel, M.L. Rosenblum, T. Mikkelsen, P.S. Yan, K.D. Ellis, W.A. Golembieski, M. Sameni, J. Rozhin, G. Ziegler, B.F. Sloane, Cathepsin B expression and localization in glioma progression and invasion, Cancer Res. 54 (23) (1994) 6027–6031.
[47] P. Matarrese, B. Ascione, L. Ciarlo, R. Vona, C. Leonetti, M. Scarsella, A.M. Mileo, C. Catricalà, M.G. Paggi, W. Malorni, Cathepsin B inhibition interferes with metastatic potential of human melanoma: an in vitro and in vivo study, Mol. Cancer 9 (1) (2010) 207, https://doi.org/10.1186/1476-4598-9-207.
[48] N.P. Withana, G. Blum, M. Sameni, C. Slaney, A. Anbalagan, M.B. Olive, B. N. Bidwell, L. Edgington, L. Wang, K. Moin, B.F. Sloane, R.L. Anderson, M. S. Bogyo, B.S. Parker, Cathepsin B inhibition limits bone metastasis in breast cancer, Cancer Res. 72 (5) (2012) 1199–1209.
[49] V. Gocheva, J.A. Joyce, Cysteine cathepsins and the cutting edge of cancer invasion, Cell Cycle 6 (1) (2007) 60–64.
[50] A. Bervar, I. Zajc, N. Sever, N. Katunuma, B.F. Sloane, T.T. Lah, Invasiveness of transformed human breast epithelial cell lines is related to cathepsin B and inhibited by cysteine proteinase inhibitors, Biol. Chem. 384 (3) (2003) 447–455.
[51] A. Ritonja, T. Popovic, V. Turk, K. Wiedenmann, W. Machleidt, Amino acid sequence of human liver cathepsin B, FEBS Lett. 181 (1) (1985) 169–172.
[52] K. Moin, N.A. Day, M. Sameni, S. Hasnain, T. Hirama, B.F. Sloane, Human tumour cathepsin B. Comparison with normal liver cathepsin B, Biochem. J. 285 (Pt 2) (1992) 427–434.
[53] Y. Yang, X. Yang, S.H. Verhelst, Comparative analysis of click chemistry mediated activity-based protein profiling in cell lysates, Molecules 18 (10) (2013) 12599–12608.
[54] L. Cianni, C.W. Feldmann, E. Gilberg, M. Gütschow, L. Juliano, A. Leitão, J. Bajorath, C.A. Montanari, Can cysteine protease cross-class inhibitors achieve selectivity? J. Med. Chem. 62 (23) (2019) 10497–10525.
[55] V.V. Nemmara, V. Subramanian, A. Muth, S. Mondal, A.J. Salinger, A.J. Maurais, R. Tilvawala, E. Weerapana, P.R. Thompson, The development of benzimidazole-based clickable probes for the efficient labeling of cellular protein arginine deiminases (PADs), ACS Chem. Biol. 13 (3) (2018) 712–722.
[56] D. Dana, J. Garcia, A.I. Bhuiyan, P. Rathod, L. Joo, D.A. Novoa, S. Paroly, K. R. Fath, E.J. Chang, S.K. Pathak, Cell penetrable, clickable and tagless activity-based probe of human cathepsin L, Bioorg. Chem. 85 (2019) 505–514.
[57] D. Dana, T.K. Das, I. Kumar, A.R. Davalos, K.J. Mark, D. Ramai, E.J. Chang, T. T. Talele, S. Kumar, Design, Synthesis, and evaluation of 2-(arylsulfonyl)oxiranes as cell-permeable covalent inhibitors of protein tyrosine phosphatases, Chem. Biol. Drug Des. 80 (4) (2012) 489–499.
[58] D. Dana, A.R. Davalos, S. De, P. Rathod, R.K. Gamage, J. Huestis, N. Afzal, Y. Zavlanov, S.S. Paroly, S.A. Rotenberg, G. Subramaniam, K.J. Mark, E.J. Chang, S. Kumar, Development of cell-active non-peptidyl inhibitors of cysteine cathepsins, Bioorg. Med. Chem. 21 (11) (2013) 2975–2987.
[59] C.A. Schneider, W.S. Rasband, K.W. Eliceiri, NIH Image to ImageJ: 25 years of image analysis, Nat. Methods 9 (7) (2012) 671–675.
[60] I.-C. Huang, B.J. Bosch, F. Li, W. Li, K.H. Lee, S. Ghiran, N. Vasilieva, T.S. Dermody, S.C. Harrison, P.R. Dormitzer, M. Farzan, P.J.M. Rottier, H. Choe, SARS coronavirus, but not human coronavirus NL63, utilizes cathepsin L to infect ACE2-expressing cells, J. Biol. Chem. 281 (6) (2006) 3198–3203.